Formation and Structure of $Rh^{(0)}$ Complexes of Phosphinine-Containing Macrocycles: EPR and DFT Investigations

Laurent Cataldo, Sylvie Choua, Théo Berclaz, and Michel Geoffroy*

Department of Physical Chemistry, 30 quai Ernest Ansermet, University of Geneva, 1211 Geneva, Switzerland

Nicolas Mézailles, Narcis Avarvari, François Mathey,* and Pascal Le Floch*

Laboratoire "Hétéroéléments et Coordination", UMR CNRS 7653, Ecole Polytechnique, 91128 Palaiseau Cedex, France

Received: November 29, 2001

Electrochemical and chemical reductions of $Rh^{(I)}$ complexes of $\mathbf{L_{P4}}$ (a macrocycle containing four phosphinine rings) and of $\mathbf{L_{P2S2}}$ (a macrocycle containing two phosphinine rings and two thiophene rings) lead, in liquid solution, to EPR spectra exhibiting large hyperfine couplings with ^{31}P nuclei. An additional coupling (27 MHz) with ^{103}Rh is detected, in the liquid state, for the spectrum obtained with $\mathbf{[L_{P2S2}Rh^{(0)}]}$; moreover, resolved ^{31}P hyperfine structure is observed in the frozen solution spectrum of this latter complex. DFT calculations performed on $Rh^{(I)}$ complexes of model macrocycles $\mathbf{L'_{P4}}$ and $\mathbf{L'_{P2S2}}$ indicate that, in these systems, the metal coordination is planar and that one-electron reduction induces a small tetrahedral distortion. The calculated couplings, especially the dipolar tensors predicted for $\mathbf{[L'_{P2S2}Rh^{(0)}]}$, are consistent with the experimental results. Although the unpaired electron is mostly delocalized on the ligands, the replacement of two phosphinines by two thiophenes tends to increase the rhodium spin density (ρ_{Rh} =0.35 for $\mathbf{[L'_{P2S2}Rh^{(0)}]}$). It is shown that coordination to Rh as well as one-electron reduction of the resulting complex provoke appreciable changes in the geometry of the macrocycle.

Introduction

Complexes of metals in low oxidation states present a considerable interest for reductive catalysis, and intense efforts are currently made to design new ligands able to complex electron-rich metal ions. In this context, compounds containing unsaturated carbon−phosphorus bonds have shown promising properties.[1,2] This is the case of phosphinines whose low lying π^* LUMO is well suited to the accommodation of extra electrons.[3] Moreover, recent progress in synthetic chemistry,[4,5] has made possible the use of macrocycles such as $\mathbf{L_{P4}}$ and $\mathbf{L_{P2S2}}$, which incorporate several phosphinine units and which are expected to provide thermodynamic stabilization [6] to the metal center.

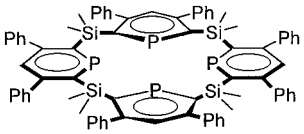

$\mathbf{L_{P4}}$

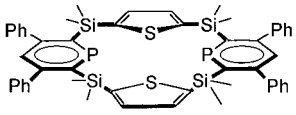

$\mathbf{L_{P2S2}}$

There are few complexes with rhodium centers in low oxidation states [7] and, as far as we know, only a single monomeric $Rh^{(0)}$ has been structurally characterized.[8] Because the chemical behavior of these paramagnetic complexes is mostly governed by the location of the unpaired electron, it is important to know how the nature of the ligand influences the contribution of the metal to the SOMO. However, due to the low stability of these complexes or, perhaps, to a too high fluxionality that limits the spectral resolution, the ^{103}Rh isotropic coupling of these rare complexes could never be directly observed in the liquid state. The geometry of $Rh^{(0)}$ complexes seems to be very sensitive to the nature of the ligands. For example, Chenier et al. [9] could trap $[Rh(CO)_4]$ in hydrocarbon matrixes at 77 K and showed that this complex is only slightly distorted from tetrahedral geometry whereas Orsini and Geiger recently found that in $[(COD)_2Rh]$ "the ligands form a ligand field around Rh which is closer to square planar than to tetrahedral".[10]

In the present study, we used the two polydentate ligands $\mathbf{L_{P4}}$ and $\mathbf{L_{P2S2}}$ to form $Rh^{(I)}$ complexes and show that their chemical or electrochemical reductions easily lead to the macrocyclic $Rh^{(0)}$ complex. EPR spectroscopy and DFT calculations were used to assess the structure of these formally d^9-rhodium compounds and, in particular, to reveal how the nature of the heterocycles (phosphinines or thiophene) affects the spin repartition.

Experimental Section

Compounds. All reactions were routinely performed under an inert atmosphere of argon or nitrogen by using Schlenk and glovebox techniques and dry deoxygenated solvents. Dry THF and hexanes were obtained by distillation from Na/benzophenone and dry $CDCl_3$ from P_2O_5. CD_2Cl_2 was dried and stored, like $CDCl_3$, on 4 Å Linde molecular sieves. Nuclear magnetic resonance spectra were recorded on a Bruker AC-200 SY spectrometer operating at 200.13 MHz for ^1H, 50.32 MHz for ^{13}C and 81.01 MHz for ^{31}P. Solvent peaks are used as internal reference relative to Me_4Si for ^1H and ^{13}C chemical shifts (ppm); ^{31}P chemical shifts are relative to a 85% H_3PO_4 external reference. Coupling constants are given in Hertz. The following abbreviations are used: s, singlet; d, doublet; t, triplet; m,

10.1021/jp014339z CCC: $22.00
Published on Web 02/28/2002

multiplet; p, pentuplet; v, virtual. IR data were collected on a Perkin-Elmer 297 spectrometer. Mass spectra were obtained at 70 eV with a HP 5989B spectrometer coupled to a HP 5980 chromatograph by the direct inlet method. Elemental analyses were performed by the "Service d'analyze du CNRS", at Gif sur Yvette, France.

Synthesis of [L_{P4}Rh][BF_4]. [$Rh(COD)_2$][BF_4] (41 mg, 0.1 mmol) and $\mathbf{L_{P4}}$[5] (122 mg, 0.1 mmol) were weighed in air and then placed under nitrogen in a Schlenk flask. CH_2Cl_2 (8 mL) was syringed in and the mixture was stirred at room temperature for 1 h. The solvent was evaporated under vacuum, and the precipitate washed with hexanes (2 × 2 mL). The title compound was collected as a red solid after drying under vacuum. Yield: 140 mg (95%). ^{31}P NMR ($CDCl_3$): δ 228.8 (d, ^1J(P − ^{103}Rh) = 144.5). ^{1}H NMR ($CDCl_3$): δ −1.10 (s, 12H, 4 × Me), 1.06 (s, 12H, 4 × Me), 7.13−7.39 (m, 44H, 8 × Ph, 4 × H_4). ^{13}C NMR ($CDCl_3$): δ 0.9 (s, 4 × Me), 3.8 (s, 4 × Me), 128.4−129.3 (m, CH of Ph), 132.4 (d, ^3J(C − P) = 5.8, C_4), 144.4 (s, $C_{3',5'}$), 151.3 (d, ^2J(C − P) = 2.7, $C_{3,5}$), 157.8 (sl, $C_{2,6}$). Anal. Calcd for $C_{76}H_{68}BF_4P_4RhSi_4$: C, 64.86; H, 4.84. Found: C, 64.69; H, 4.72.

Synthesis of [L_{P2S2}Rh][BF_4]. [$Rh(COD)_2$][BF_4] (41 mg, 0.1 mmol) and $\mathbf{L_{P2S2}}$[5] (89 mg, 0.1 mmol) were weighed in air and then placed under nitrogen in a Schlenk flask. CH_2Cl_2 (8 mL) was syringed in and the mixture was stirred at room temperature for 1 h. The volume was reduced under vacuum, and the complex was precipitated with hexane (5 mL). The pale orange solid was collected on a fine frit and then washed with hexane (2 × 2 mL) and dried under vacuum. Yield: 100 mg (93%). ^{31}P NMR ($CDCl_3$): δ 228.0 (d, ^1J(P − ^{103}Rh) = 146.8); ^{1}H NMR ($CDCl_3$): δ −0.25 (s, 6H, 2 × Me), 0.89 (s, 6H, 2 × Me), 7.36−7.52 (m, 26H, 4 × Ph, 2 × thiophene, 2 × H_4); ^{13}C NMR ($CDCl_3$): δ −1.75 (s, 2 × Me), 5.0 (s, 2 × Me), 129.0−129.4 (m, CH of Ph), 132.1 (vt, ΣJ(C − P) = 33.4, C_4), 139.8 (s, $C_{3,4}$ thiophene), 144.2 (m, ΣJ(C − P) = 10.5, $C_{3'\text{ and }5'}$), 150.8 (pt, ΣJ(C − P) = 9.0, $C_{3,5}$), 152.7 (vt, ΣJ(C − P) = 22.1, $C_{2,5}$ thiophene) 158.5 (vt, ΣJ(C − P) = 13.2, $C_{2,6}$); Anal. Calcd for $C_{50}H_{50}BF_4P_2RhS_2Si_4$: C, 55.65; H, 4.67. Found: C, 55.90; H, 4.81.

EPR. EPR spectra were recorded on a Bruker 200 D and a Bruker 300 spectrometers (X-band, 100 kHz field modulation) equipped with a variable temperature attachment. Solvents, THF and CH_2Cl_2, were carefully dried (on Na and P_2O_5 respectively) and degassed. Reactions on potassium mirrors were carried out under high vacuum in sealed tubes. Electrochemical reductions were performed under a nitrogen atmosphere. Liquid solution spectra were simulated using a homemade program which takes into account the broadening of the lines caused by an incomplete averaging of the dipolar hyperfine coupling. Optimization and simulation of the frozen solution spectra were carried out with a program[11] based on the Levenberg−Marquardt algorithm, which compares the experimental transitions with those calculated by second-order perturbation theory.

DFT Calculations. Calculations of the optimized geometries and of the hyperfine coupling tensors were performed with the Gaussian 98 package:[12] spin-unrestricted calculations, B3LYP functional.[13] For the ligand's atoms, the 6-31G* and 6-31+G* basis sets were used for calculations on the $Rh^{(I)}$ and the $Rh^{(0)}$ complexes, respectively. The Stevens−Basch−Krauss ECP triple split basis (SBK)[14], recently used by Sundermann and Schoeller [15]to calculate the electronic structure of transition metal complexes of a phosphorus-containing ligand, was used for rhodium. The optimized structures were characterized by harmonic frequency analysis as minima (all frequencies real). The Molekel program was used for the representation of the MO. [16]

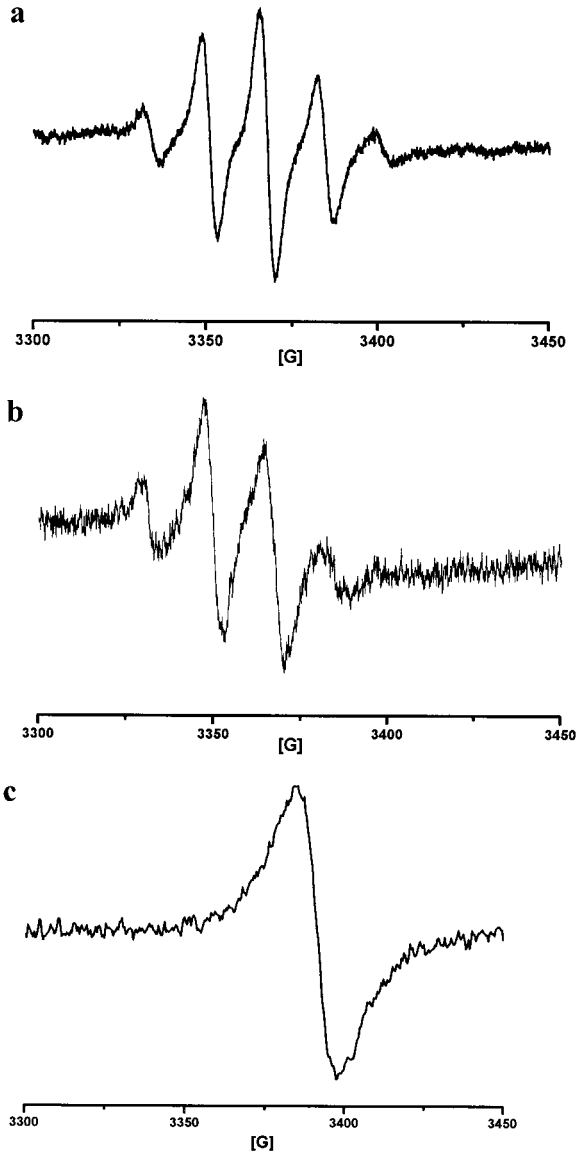

Figure 1. EPR spectra obtained after electrochemical reduction of a solution of **[L_{P4} Rh][BF_4]** in CH_2Cl_2. a: spectrum recorded at 300 K ($\nu_{klystron}$ = 9435.3 MHz), b: spectrum recorded at 200 K ($\nu_{klystron}$ = 9435.6 MHz), c: spectrum recorded at 120 K ($\nu_{klystron}$ = 9438.3 MHz).

Results

EPR Spectra. No EPR spectrum could be obtained by electrochemical or chemical reduction of the noncomplexed macrocycles $\mathbf{L_{P4}}$ or $\mathbf{L_{P2S2}}$ in solution in THF or CH_2Cl_2. A solution of [$\mathbf{L_{P4}}$ **Rh] [BF_4]** in CH_2Cl_2 (concentration higher than 10^{-2} mol·l^{-1}) turned to red when electrochemically reduced at room temperature and led to the spectrum shown in Figure 1a. The five signals separated by 16.7 G [17] are centered around g = 2.0016, their intensity distribution (1−4−6−4−1) clearly indicates hyperfine interaction with four equivalent ^{31}P nuclei. The same spectrum was obtained by reacting a solution of **[L_{P4}Rh] [BF_4]** in CH_2Cl_2 on a potassium or a sodium mirror at room temperature. The unsymmetrical broadening of the lines occurred on lowering the temperature; this effect, due to incomplete averaging of the anisotropies in the g and hyperfine tensors, is similar to previous observations on [$Rh(dppe)_2$][18] We

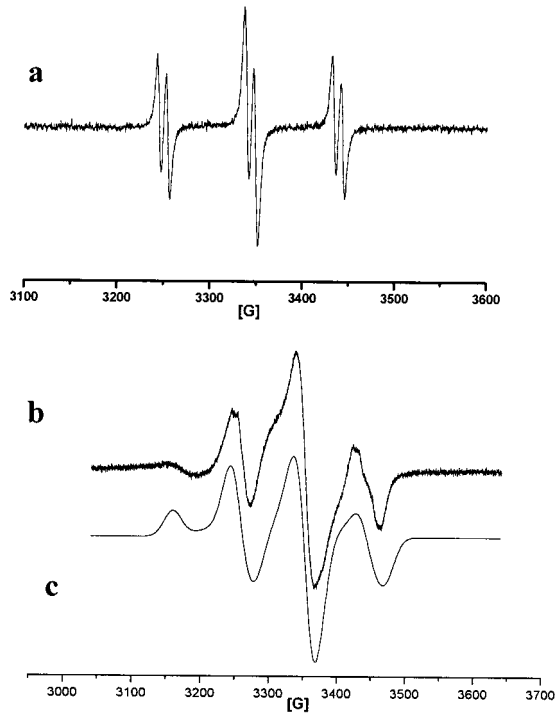

Figure 2. EPR spectra obtained after electrochemical reduction of a solution of [$\mathbf{L_{P2S2}Rh}$] [$\mathbf{BF_4}$] in CH_2Cl_2. a: spectrum recorded at 300 K, b: spectrum recorded at 130 K, c: simulation of the frozen solution spectrum.

could simulate the spectra at various temperatures by expressing this broadening as a power series in the nuclear spin quantum numbers. At 200 K, the broadening of the high field line became so large that only four lines were detected (Figure 1b); finally, at120 K, a single large signal, without any resolved structure was recorded (Figure 1c). These spectral changes with temperature were all reversible.

Although no EPR signal could be observed by reacting a solution of $\mathbf{[L_{P2S2}Rh][BF_4]}$ in CH_2Cl_2 (5×10^{-3} or 10^{-2} mol·l^{-1}) with K or Na mirrors, these solutions in CH_2Cl_2 (or THF) became red on electrochemical reduction and led to the spectrum shown in Figure 2a. The same spectrum was obtained by reducing a solution of $\mathbf{[L_{P2S2}Rh][BF_4]}$ in THF (5×10^{-3} mol·l^{-1}) with Na naphthalenide. This spectrum is characterized by an hyperfine splitting of 96 G with two equivalent ^{31}P nuclei and a splitting of 9.6 G with an additional spin 1/2 nucleus. Clearly, this additional coupling is due to ^{103}Rh (natural abundance 100%). A broadening of the signals is observed when the temperature decreases, and, as shown in Figure 2b, at 130 K, the very anisotropic frozen solution spectrum is composed of four lines. This spectrum was simulated by adding the ^{31}P and ^{103}Rh isotropic coupling constants measured in liquid solutions to the dipolar tensors obtained from DFT calculations (vide infra) and by optimizing the *g* tensor. As shown in Figure 2c, the resulting spectrum satisfactory simulates the experimental one. Subsequent optimizations of the dipolar tensors did not lead to an appreciable improvement of this simulation. The EPR parameters obtained for $\mathbf{[L_{P4}Rh^{(0)}]}$ and $\mathbf{[L_{P2S2}Rh^{(0)}]}$ are given in Table 1.

DFT Calculations. Calculations have been carried out on the model systems $\mathbf{[L'_{P4}Rh^{(I)}]}$ and $\mathbf{[L'_{P2S2}Rh^{(I)}]}$, which, in contrast to the real molecules, have neither phenyl group bound to the phosphinine rings nor methyl group bound to silicon atoms.

Optimization of $\mathbf{[L'_{P4}Rh^{(I)}]}$ has been performed assuming S_4 symmetry. The resulting geometries are shown in Figure 3, whereas the corresponding geometrical parameters are given in Table 2 together with the values obtained from the crystal structure[1] of $\mathbf{[L_{P4}Rh^{(I)}]}$. The accord between these two sets of values is quite satisfactory: the calculated Rh−P distances as well as the calculated P−Rh−P angles are consistent with the experimental values. For both structures, the phosphinine rings are planar and the angle $\theta_{\text{phosphinine}}$ between the normals to two opposed phosphinine rings is close to 70°. As indicated by the angle ξ formed by the normals to the planes P1RhP4 and P2RhP3, the rhodium coordination is perfectly square planar in the calculated structure, whereas, probably due to some packing effect, it is slightly distorted ($\xi = 11°$) in the crystal.

All our efforts for growing crystals of $\mathbf{[L_{P2S2}Rh^{(I)}]}$ suitable for X-ray diffraction remained unsuccessful; however, the results obtained for $\mathbf{[L'_{P4}Rh^{(I)}]}$ indicate that DFT calculations can confidently be used for predicting the structure of $\mathbf{[L_{P2S2}Rh^{(I)}]}$. The geometry of $\mathbf{[L'_{P2S2}Rh^{(I)}]}$ has been optimized by assuming C_2 symmetry and is shown in Figure 3, whereas the corresponding parameters are also given in Table 2. The Rh−S distances are similar to those measured (2.32 Å) in thiaporphyrin complexes.[19]

The optimized structures of the one-electron-reduction products, $\mathbf{[L'_{P4}Rh^{(0)}]}$ and $\mathbf{[L'_{P2S2}Rh^{(0)}]}$ are given in Table 2. For these two compounds, no crystal structure is of course available and the reliability of the DFT calculations can be checked only by comparing experimental and calculated hyperfine interactions. The hyperfine parameters[20] calculated for $\mathbf{[L'_{P4}\ Rh^{(0)}]}$ and $\mathbf{[L'_{P2S2}Rh^{(0)}]}$ are given in Table 3.

For both complexes, the accord between the ^{31}P isotropic coupling constants and the EPR values is quite acceptable. As explained above, the fact that the experimental frozen solutions spectra could be simulated by using the ^{31}P and ^{103}Rh experimental isotropic couplings together with the calculated ^{31}P and ^{103}Rh dipolar tensors indicates that the calculated anisotropic couplings are consistent with the EPR results.

Discussion

The structure of a complex containing a metal ion ligated by a macrocycle mainly results from a balance between two principal factors: (1) the size of the metal ion and its preferred coordination geometry in the considered oxidation state, (2) the ligand properties and steric constraints of the macrocycle. Here, we will examine the structural changes induced by the replacement, in the macrocycle, of two phosphinine rings by two thiophene rings and will try to rationalize the modifications caused by the one-electron reduction of these complexes.

We first recall some geometry characteristics[5] obtained from the crystal structure of the two macrocycles $\mathbf{L_{P4}}$ and $\mathbf{L_{P2S2}}$ and illustrated in Figure 4: in both compounds, the phosphorus or/and sulfur atoms are coplanar and the planes of two opposite rings are almost parallel. In $\mathbf{L_{P4}}$ and $\mathbf{L_{P2S2}}$, two opposite phosphinine rings are oriented perpendicular to the $P_1P_2P_3P_4$ (or $P_1S_2P_3S_4$) plane while the two other phosphinine rings in $\mathbf{L_{P4}}$ and the two thiophene rings in $\mathbf{L_{P2S2}}$ are oriented parallel to this plane.

Despite the coplanarity of the phosphorus and sulfur atoms in the free macrocycle, the fact that pairs of ligand rings lie in perpendicular planes does not seem propitious for a planar coordination of the metal ion. Nevertheless, as shown by the calculated angle ξ ($\xi = 0°$) formed by the normals to the planes P1RhP4 and P2RhP3, the overall geometry of rhodium is square planar in $\mathbf{[L'_{P4}\ Rh^{(I)}]}$; in $\mathbf{[L'_{P2S2}Rh^{(I)}]}$, however, the value of

TABLE 1: Experimental g and Hyperfine (MHz) Parameters

	$g_{average}$ (liquid)	g-tensor (frozen)	$^{31}P-A_{iso}$ (liquid)	^{31}P-tensor[a] (frozen)	$^{103}Rh-A_{iso}$ (liquid)	103Rh-tensor[a] (frozen)
$[L_{P4}Rh^{(0)}]$	2.0016			(4 ^{31}P nuclei)		
			49			
$[L_{P2S2}][Rh^{(0)}]$				(2 ^{31}P nuclei)		
	2.018		271		27	
		$\begin{bmatrix} 2.0135 & 0 & 0 \\ 0 & 2.0018 & 0 \\ 0 & 0 & 2.0797 \end{bmatrix}$		$\begin{bmatrix} 276 & -15 & \mp 16 \\ -15 & 289 & \pm 38 \\ \mp 16 & \pm 38 & 274 \end{bmatrix}$		$\begin{bmatrix} 24 & 0 & 0 \\ 0 & 25 & 0 \\ 0 & 0 & 30 \end{bmatrix}$

[a] These hyperfine tensors used for the simulation were obtained by adding the isotropic part (measured on the liquid solution spectrum) to the dipolar tensor (obtained from the DFT calculations); the sign combinations correspond to the orientations of the two ^{31}P dipolar tensors.

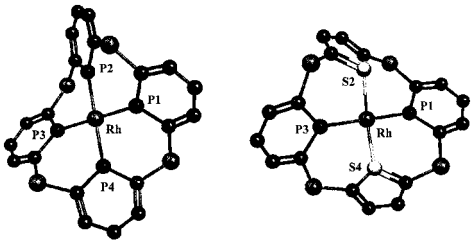

[L'$_{P4}$ Rh$^{(I)}$] **[L'$_{P2S2}$Rh$^{(I)}$]**

Figure 3. DFT optimized geometries of **[L′$_{P4}$Rh$^{(I)}$]** and **[L′$_{P2S2}$Rh$^{(I)}$]**.

TABLE 2: Experimental and Calculated Geometries (distances in Å, Angles in Degres)

	$[L_{P4}Rh^{(I)}]$ (crystal)	$[L'_{P4}Rh^{(I)}]$ (DFT)	$[L'_{P4}Rh^{(0)}]$ (DFT)	$[L'_{P2S2}Rh^{(I)}]$ (DFT)	$[L'_{P2S2}Rh^{(0)}]$ (DFT)
Rh−P	2.270	2.320	2.311	2.346	2.349
Rh−S				2.365	2.433
P2−Rh−P1	90.8	90.0	90.1		
P−Rh−S				94.1 (86.5)	88.1 (93.9)
P2−Rh−P3	171.5	179.9	174.0	174.7	168.1
S−Rh−S				166.0	159.9
ξ (coordination angle)	11.6	0.0	8.4	15.2	22.6
$\theta_{phosphinine}$	77.8°	67.4	66.1	56.1	57.1
$\theta_{thiophene}$				79.8	83.0
$\chi_{phosphinine}$	82−87	90.0	79.7	86.0	70.8
$\chi_{thiophene}$				40.8	38.8

ξ: angle between the normals to the planes P1RhP4 and P2RhP3 for **[L$_{P4}$Rh$^{(I)}$]**, **[L′$_{P4}$Rh$^{(I)}$]**, and **[L′$_{P4}$Rh$^{(0)}$]** and between the normals to the planes P1RhS4 and S2RhP3 for **[L′$_{P2S2}$Rh$^{(I)}$]**and **[L′$_{P2S2}$Rh$^{(0)}$].** $\theta_{phosphinine}$: angle between the normals to the CPC planes of two opposite phosphinine rings. $\theta_{thiophene}$: angle between the normals to the planes of two thiophene rings. $\chi_{phosphinine}$: angle between the normal to the phosphinine CPC plane and the corresponding Rh−P direction. $\chi_{thiophene}$: angle between the normal to the thiophene ring (CSC plane) and the Rh−S direction

the corresponding ξ angle (ξ: angle formed by the normals to P1RhS4 and S2RhP3 = 15.2°) indicates that the presence of the thiophene rings induces a small tetrahedral distortion in the rhodium coordination. In both complexes the P−Rh bond lengths are close to 2.33 Å which is slightly longer than the value measured in the crystal of **[L$_{P4}$ Rh$^{(I)}$]**. Chelation of the Rh^+ ions provokes drastic changes in the geometry of the two macrocycles: as, expected the distances between two opposite phosphorus or sulfur atoms decrease, but the inter-phosphorus distance[21] is considerably more affected (P..P variation = 1.14 and 1.562 Å for **[L′$_{P4}$ Rh$^{(I)}$]** and **[L′$_{P2S2}$Rh$^{(I)}$]**, respectively) than that of the inter-sulfur distance (S..S variation = 0.106 Å). In **[L′$_{P4}$ Rh$^{(I)}$]**, each Rh−P direction is perpendicular to the normal to the corresponding phosphinine plane ($\chi_{phosphinine}$ = 90°), in accord with a phosphorus coordination along the C_{para}...P direction, and the angle $\theta_{phosphinine}$ between the normals to two opposite phosphinine rings is equal to ∼67° instead of 0° in the free macrocycle. In **[L′$_{P2S2}$Rh$^{(I)}$]**, in contrast to the Rh−P directions which are also almost perpendicular to the associated CPC plane ($\chi_{phosphinine}$ = 86°), the Rh−S directions make an angle $\chi_{thiophene}$ of 41° with the normal to the CSC plane of the corresponding thiophene ring; this result confirms that the thiophene binds the metal ion through a pyramidal sulfur in a η^1 (S) fashion[22,23] as in palladium (II) complexes of thiaporphyrins [24] or as in $[Rh(CO)L][ClO_4]$ (where L represents 2,5-Bis(2-(diphenylphosphino) ethyl)thiophene[25]). This coordination leads to a small folding (∼5°) of the thiophene ring which adopts an ≪ envelope ≫ conformation (with the sulfur atom slightly outside the mean plane of the ring) and to an inter-thiophene angle $\theta_{thiophene}$ equal to ∼80° ($\theta_{thiophene}$ = angle between the normals to the CSC planes) instead of the alignment ($\theta_{thiophene}$ = 0°) observed for the free macrocycle **L$_{P2S2}$**. Replacement of two phosphinines in **[L′$_{P4}$Rh$^{(I)}$]** by two thiophenes moderately affects the relative orientation of the two opposite phosphinines and causes a ∼10° decrease in the $\theta_{phosphinine}$ angle.

As shown in Table 2, for **[L′$_{P4}$Rh$^{(I)}$]** and **[L′$_{P2S2}$Rh$^{(I)}$]** the one-electron reduction causes a small tetrahedral distortion which is revealed by an increase of about 8° in the values of ξ. For both reduced complexes, neither the P−Rh distances nor the mutual orientations of two opposite phosphinines or two opposite thiophenes seem to be affected by the reduction (the variations of $\theta_{phosphinine}$ or $\theta_{thiophene}$ is less than 3°). Nevertheless, although the phosphinine ring remains planar, a small pyramidalisation of the phosphorus coordination occurs: the $\chi_{phosphinine}$ angle decreases of ∼10° and of ∼15° when passing from **[L′$_{P4}$Rh$^{(I)}$]** to **[L′$_{P4}$Rh$^{(0)}$]** and from **[L′$_{P2S2}$Rh$^{(I)}$]** to **[L′$_{P2S2}$Rh$^{(0)}$]** respectively. Modifications involving the thiophene moieties remain modest: the folding of this ring as well as the sulfur pyramidalisation seem to be hardly affected by the reduction process.

As visualized on Figure 5a, in **[L′$_{P4}$Rh$^{(0)}$]**, the ligand orbitals largely participate in the SOMO; in fact, only 10% of the unpaired electron is localized on the metal (total atomic spin density on rhodium = 0.094, with a large contribution of the $d_{x^2-y^2}$ orbital), whereas ∼20% is delocalized in a π^* type orbital of each phosphinine with a total atomic spin density of 0.1 on each phosphorus atom (gross orbital spin population on phosphorus: ρ_{pz} = 0.09, ρ_s = 0.003).

In **[L′$_{P2S2}$Rh$^{(0)}$]**, the unpaired electron is mainly delocalized on the rhodium and the two phosphorus atoms (total atomic spin densities on each atom: ρ_P = 0.12, ρ_{Rh} = 0.355), whereas the spin density on each sulfur remains very small (ρ_S = 0.015). As visualized on Figure 5b, the rhodium d_{x2-y2} and phosphorus s and p_π atomic orbitals mainly contribute to the SOMO. The participation of the phosphorus s orbital (gross orbital spin population $\rho_S(P)$ = 0.043) is clearly superior to that found for **[L′$_{P4}$Rh$^{(0)}$]** and explains the large difference in the phosphorus

TABLE 3: Calculated Hyperfine Interactions for [L′$_{P4}$Rh$^{(0)}$]and [L′$_{P2S2}$Rh$^{(0)}$]

	^{103}Rh coupling (MHz)					^{31}P coupling (MHz)			
	dipolar tensor					dipolar tensor			
		eigenvectors					eigenvectors[a]		
complex	eigenvalues	λ	μ	ν	A_{iso}	eigenvalues	λ	μ	ν
[L′$_{P4}$ Rh$^{(0)}$]	0.71	0.0	0.0	1.0	53	35	0.3631	−0.3953	0.8437
	−0.35					−22	0.1564	0.9185	0.3631
	−0.35					−12	0.9185	0.000	−0.3954
[L′$_{P2S2}$Rh$^{(0)}$]	3.4	0.0	0.0	1.0	203	52.3	−0.3550	0.5293	0.7706
	−1.0					−39.4	0.1259	0.8439	−0.5216
	−2.3					−12.8	0.9264	0.0881	0.3662

[a] For **[L′$_{P4}$Rh$^{(0)}$],** the eigenvectors of the three other ^{31}P dipolar tensors are given by: $-\lambda,\nu$; $-\lambda, -\mu, \nu$; $-\mu, \lambda,\nu$. For **[L′$_{P2S2}$Rh$^{(0)}$]**, the eigenvector of the ^{31}P tensor is given by: $-\lambda, -\mu, \nu$.

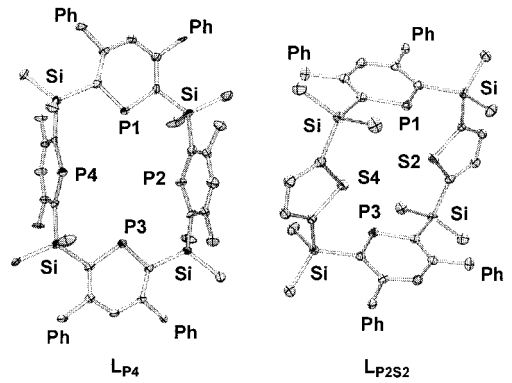

Figure 4. ORTEP view of the two macrocycles $\mathbf{L_{P4}}$ and $\mathbf{L_{P2S2}}$.

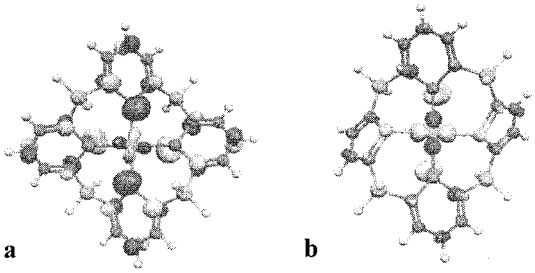

Figure 5. Representation of the SOMO of **[L′$_{P4}$Rh$^{(0)}$]** and **[L′$_{P2S2}$Rh$^{(0)}$]**.

couplings observed on the liquid solution spectra of **[L$_{P4}$Rh$^{(0)}$]** and **[L$_{P2S2}$Rh$^{(0)}$]**.

Although it is not possible to directly estimate the ^{103}Rh isotropic coupling[20] from our DFT calculations, the fact that the metal spin density is appreciably larger for **[L′$_{P2S2}$Rh$^{(0)}$]** than for **[L′$_{P4}$Rh$^{(0)}$]** agrees with the fact that an isotropic coupling was detected with **[L$_{P2S2}$Rh$^{(0)}$]** and not with **[L$_{P4}$Rh$^{(0)}$]**. The deviation of the hyperfine eigenvector ^{31}P−T$_{max}$ from the normal n to the associated CPC plane is more marked for **[L′$_{P2S2}$Rh$^{(0)}$]** ($(n, ^{31}\text{P}-\text{T}_{max}) = 45°$) than for **[L′$_{P4}Rh^{(0)}$]** ($n$, ^{31}P−T$_{max}$) = 31°). This deviation probably results from two factors: the pyramidalization of the phosphorus atom (as shown by the $\chi_{phosphinine}$ value) and the contribution of the spin localized in the rhodium orbitals to the ^{31}P dipolar tensor.

Although the spin density on the sulfur atom is quite small ($\rho_S = 0.015$), the delocalization of the unpaired electron on the carbon atoms of the thiophene ring is not negligible and the total spin density on each thiophene is equal to 0.09. This delocalization of the unpaired electron on both the metal ion (35%) and the thiophene-containing macrocylic ligand is reminiscent of previous observations [26] on the one-electron reduction product of nickel(II) thiaporphyrin whose SOMO involved comparable contributions of ligand and metal characters.

The g-tensor measured for **[L$_{P2S2}$Rh$^{(0)}$]** exhibits some departure from axial symmetry, nevertheless by neglecting the ≪rhombic≫ component, it corresponds to $g_e \leq g_\perp < g_{//}$. This is in accord with a d^9 configuration with the unpaired electron in a $d_{x^2-y^2}$ orbital. The *g*-anisotropy is however rather small and is consistent with a spin delocalization onto the ligands and a slight tetrahedral distortion of the metal coordination in good accordance with the DFT optimized structure. However, our attempts to calculate the *g* tensor by using the DFT method [27] led to a still smaller anisotropy ($g_1 = 2.012$, $g_2 = 2.016$, $g_3 = 2.0287$).

Due to the considerable interest of monomeric d^9 species of rhodium with phosphorus ligands in the field of homogeneous catalysis, numerous efforts have been made to assign the structure of these complexes. It was proposed that [(PPh$_3$)$_4$Rh$^{(0)}$] [28] or [(PPh$_3$)$_3$(CO) Rh$^{(0)}$] [29] adopt tetrahedral structures whereas, a square planar structure [30] was attributed to [(Pr^{i}O)$_3$P)$_4$Rh$^{(0)}$]. However, the EPR spectra were often very complex, and, in many cases, the hyperfine structure was not clearly resolved. Moreover, different mechanisms were proposed for the electrochemical reduction of d^8 square planar complexes of rhodium containing phosphorus ligands,[31,32] These difficulties led to conflicting reports. For example, [(Pr^{i}O)$_3$P)$_4$Rh$^{(0)}$] was also reported to be tetrahedral with a tetragonal compression.[33] The only case where geometry could be determined without any ambiguity is [Rh(tropp^{ph})$_2$] where the rhodium atom is coordinated to two phosphines (in cis position) and two carbon−carbon double bonds; from the crystal structure, Grützmacher and al.[34] showed that, in this complex, the rhodium coordination is intermediate between tetrahedral and square planar geometry and is characterized by a ξ angle equal to 43°. This is quite larger than the ξ value (23°) calculated for our two phosphorus-containing complexes **[L′$_{P2S2}$Rh$^{(0)}$]**; the complex with two phosphinines is more planar than the complex with two phosphines and the difference of structure is clearly visible from the large difference in the isotropic ^{31}P couplings: A_{iso}= 69.5 MHz for [Rh(tropp^{ph})$_2$] and 259 MHz for **[L$_{P2S2}$Rh$^{(0)}$].**

Concluding Remark

The ability of phosphinine-containing macrocycles to stabilize metal ion in low oxidation states is confirmed by the easy one-electron reduction observed for **[L$_{P4}$Rh$^{(I)}$]** and **[L$_{P2S2}$Rh$^{(I)}$]**. As shown by joint EPR and DFT investigations, in these complexes, the nature of the coordinating heteroatoms and the oxidation state of the system moderately influence the coordination geometry of the rhodium and have an appreciable effect on the geometry of the macrocycle. The coordination of Rh$^{(0)}$ in the

reduced complexes is almost planar with the unpaired electron largely delocalized on the heterocycles; nevertheless, the replacement of two phosphinines by two thiophene rings tends to increase the spin density on the rhodium atom.

Acknowledgment. The authors thank the Swiss National Science Foundation, the CNRS, and the Ecole Polytechnique (Palaiseau) for financial support.

References and Notes

(1) Avarvari, N.; Mézailles, N.; Ricard, L.; Le Floch, P.; Mathey. F. *Science* **1998**, *289*, 1587.

(2) Jouaiti, A.; Geoffroy, M.; Terron, G.; Bernardinelli, G. *J. Am. Chem. Soc.* **1995**, *117*, 2251.

(3) Mézailles, N.; Avarvari, N.; Maigrot, N.; Ricard, L.; Mathey, F.; Le Floch, P.; Cataldo, L.; Berclaz, T.; Geoffroy, M. *Angew. Chem., Int. Ed.* **1999**, *38*, 3194.

(4) Mézailles, N.; Mathey, F.; Le Floch, P. *Progress in Inorganic Chemistry*; Karlin, K. D. Ed., 2001, vol *49*, 455.

(5) Avarvari, N.; Maigrot, N.; Ricard, L.; Mathey, F.; le Floch, P. *Chem. Eur. J.* **1999**, *5*, 2109.

(6) Constable, E. C. In *Metals and Ligand Reactivity*: Wiley VCH: Weinheim, 1996.

(7) See for example: (a) Kunin, A. J.; Nanni, E. J.; Eisenberg, R. *Inorg. Chem.* **1985**, *24*, 1852. (b) Bogdanovic, B.; Leitner, W.; Six, C.; Wilczok, U.; Wittmann, K. *Angew. Chem., Int. Ed. Engl.* **1997**, *36*, 500. (c) Mézailles, N.; Rosa, P.; Mathey, F.; Le Floch. P. *Organometallics* **2000**, *19*, 2941.

(8) Schönberg, H.; Boulmaaz, S.; Wörle, M.; Liesum, L.; Schweiger, A.; Grützmacher, H. *Angew. Chem., Int. Ed. Engl.* **1998**, *37*, 1423.

(9) Chenier. J. H. B.; Histed, M.; Howard, J. A.; Joly, H. A.; Morris, H.; Mile, B. *Inorg. Chem.* **1989**, *28*, 4114.

(10) (a) Orsini, J.; Geiger, W. E. *J. Electroanalytical Chem.* **1995**, *380*, 83. (b) Orsini, J.; Geiger, W. E. *Organometallics* **1999**, *18*, 1854.

(11) Soulié, E.; Berclaz, T.; Geoffroy, M. *AIP Conference Proceedings 330, Computational Chemistry*, Bernardi, F. and Rivail J−L, Eds, **1996**, 627.

(12) Frisch, M. J.; Trucks, G. W.; Schlegel, H. B.; Scuseria, G. E.; Robb, M. A.; Cheeseman, J. R.; Zakrzewski, V. G.; Montgomery, J. A.; Stratmann, R. E.; Burant, J. C.; Dapprich, S.; Millam, J. M.; Daniels, A. D.; Kudin, K. N.; Strain, M. C.; Farkas, O.; Tomasi, J.; Barone, V.; Cossi, M.; Cammi, R.; Mennucci, B.; Pomelli, C.; Adamo, C.; Clifford, S.; Ochterski, J.; Petersson, G. A.; Ayala, P. Y.; Cui, Q.; Morokuma, K.; Malick, D. K.; Rabuck, A. D.; Raghavachari, K.; Foresman, J. B.; Cioslowski, J.; Ortiz, J. V.; Stefanov, B. B.; Liu, G.; Liashenko, A.; Piskorz, P.; Komaromi, I.; Gomperts, R.; Martin, R. L.; Fox, D. J.; Keith, T.; Al-Laham, M. A.; Peng, C. Y.; Nanayakkara, A.; Gonzalez, C.; Challacombe, M.; Gill, P. M. W.; Johnson, B. G.; Chen, W.; Wong, M. W.; Andres, J. L.; Head-Gordon, M.; Replogle, E. S.; Pople, J. A. *Gaussian 98 (Revision A.7)*, Gaussian, Inc., Pittsburgh, PA, 1998.

(13) Becke, A. D. *J. Chem. Phys.* **1993**, *98*, 5648.

(14) Stevens, W.; Basch, H.; Krauss, J. *J. Chem. Phys.* **1984**, *81*, 6026.

(15) Sundermann, A.; Schoeller, W. W. *J. Am. Chem. Soc.* **2000**, *122*, 4729.

(16) Flukiger, P. Development of Molecular Graphics Package MOLEKEL, Ph.D. Thesis, University of Geneva, Switzerland, 1992.

(17) 10 G = 1mT.

(18) Mueller, K. T.; Kunin, A. J.; Greiner, S.; Henderson, T.; Kreilick, R. W.; Eisenberg, R. *J. Am. Chem. Soc.* **1987**, *109*, 6313.

(19) Latos-Grazynski, L.; Lisowski, J.; Olmstead, M. M.; Balch, A. L. *Inorg. Chem.* **1989**, *18*, 3328.

(20) The basis set used for rhodium (ref 14) is not appropriate for calculation of the Fermi contact interaction (effective core potential instead of all-electron calculation), therefore the ^{103}Rh isotropic coupling could not be calculated.

(21) The decrease of the P..P distance is calculated as the difference between the longest P..P distance obtained from the crystal structure of $\mathbf{L_{P4}}$ (or $\mathbf{L_{P2S2}}$) and the DFT calculated P..P distance in $\mathbf{[L'_{P4}\ Rh^{(I)}]}$ (or $\mathbf{[L'_{P2S2}Rh^{(I)}]}$). An analogous calculation leads to the decrease of the S..S distance. The P..P decrease between the distance measured in $\mathbf{L_{P4}}$ (crystal) and $\mathbf{[L_{P4}Rh^{(I)}]}$ (crystal) is equal to 1.27 Å.

(22) Rauchfuss, T, B. *Progress in Inorganic Chemistry*; Lippard, J., Ed.; John Wiley & Sons: New York, 1991; Vol. 39, p 260.

(23) Angelici, R. J. *Organometallics* **2001**, *20*, 1259.

(24) Latos-Grazynski, L.; Lisowski, J.; Chmielewski, P.; Grzeszczuk, M.; Olmstead, M. M.; Balch, A. L. *Inorg. Chem.* **1994**, *33*, 192.

(25) Alvarez, M.; Lugan, N.; Mathieu, R. *Inorg. Chem.* **1993**, *32*, 5652.

(26) Chmielewski, P. J.; Latos-Grazynski, L.; Pacholska, E. *Inorg. Chem.* **1994**, *33*, 1992.

(27) The *g*-tensor was calculated with the Amsterdam Density Functional (ADF) program (Baerends, E. J.; Ellis, D. E.; Ros, P. *Chem. Phys.* **1973**, *2*, 42; Velde, G.; Baerends, E. J. *J. Comput. Phys.* **1992**, *99*, 84.). General Gradient Approximation with gradient correction (BP). Standard basis set IV/ZORA in ADF. Calculations were performed with the geometry optimized from Gaussian (see experimental part).

(28) Pilloni, G.; Valcher, S.; Martelli, M. *J. Electroanal. Chem.* **1972**, 40, 63.

(29) Pilloni, G.; Vecchi, E.; Martelli, M. *J. Electroanal. Chem.* **1973**, *45*, 483.

(30) Pilloni, G.; Zotti, G.; Zecchin, S. *J. Organomet. Chem.* **1986**, *317*, 357.

(31) Sofranko, J. A.; Eisenberg, R.; Kampmeier, J. A. *J. Am. Chem. Soc.* **1979**, *101*, 1044.

(32) Pilloni,. G.; Zotti, G.; Martelli, M. *Inorg. Chem.* **1982**, *21*, 1284.

(33) George, G. N.; Klein, S. I.; Nixon, J. F. *Chem. Phys. Lett.* **1984**, *108*, 627.